RESEARCH REPORT

VTT-R-00140-26

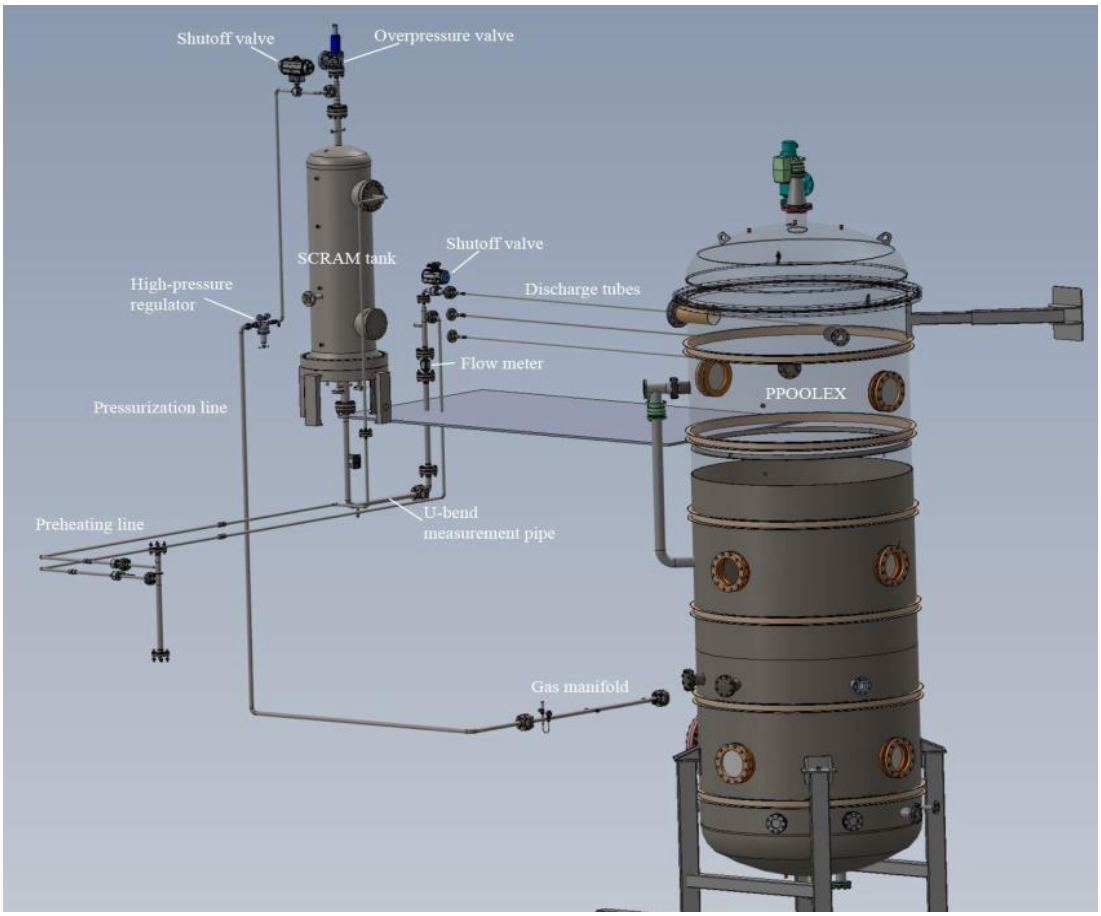

Computational Modeling of a Critical Flow Test Facility

Authors: Afeef Murad, Joona Kurki, Tatu Hovi

Confidentiality: VTT Public

VTT

beyond the obvious

Report's title	
Computational Modeling of a Critical Flow Test Facility	
Customer, contact person, address	**Order reference**
SAFER2025	SAFER 2025
Project name	**Project number/Short name**
Computational Modeling of Thermal-Hydraulic Phenomena	141364/THEME
Author(s)	**Pages**
Afeef Murad, Joona Kurki, Tatu Hovi	13/–
Keywords	**Report identification code**
Choke flow, two-phase flow, nuclear thermal-hydraulics system codes	VTT-R-00140-26

Summary

A new separate effect test facility called CRAFTY (Critical Flow Test facility) has been recently constructed at LUT (Lappeenranta University of Technology) for studying the critical flow phenomenon in geometries characterized by very large length-to-diameter ratios. From the point of view of safety analysis of nuclear power plants, such geometries are important in scenarios such as steam generator tube rupture, or small-break loss of coolant accidents. In this work, a computational model of CRAFTY is created to analyze and interpret experimental data obtained from the facility, and to study the modeling basis of critical flows applied in system-scale safety assessment tools in general. The model is built from ground up without relying on any existing simulation tool but considering the typical modeling choices applied in system-scale thermal hydraulic codes. The aim of the chosen approach is for one part to ensure that all aspects of the modeling problem are properly considered, and for one part to minimize the risk that the inherent complexity of a system-scale safety code would have an adverse effect on the modeling. The basic modeling approach based on the one-dimensional two-fluid formalism and a set of constitutive equations developed specifically for the CRAFTY test facility are presented in detail and their applicability discussed. A fully-implicit solution approach employed for fast and robust solution of the equation set is presented. Different approaches for modeling of flow choking are assessed, and their reliability discussed.

Confidentiality	VTT Public

Espoo 15.08.2025

Written by	**Reviewed by**
Afeef Murad,	Tatu Hovi,
Research Scientist	Research Scientist

VTT's contact address

VTT Technical Research Centre of Finland Ltd, P.O. Box 1000, FI-02044 VTT, FINLAND

Distribution (customer and VTT)

by email to SAFER2028 reference group 4 (Eero Virtanen, STUK; Miikka Lehtinen, STUK; Timo Toppila, Fortum; Esa Ahtinen, Fortum; Tommi Rämä, Fortum; Mikko Leminen, TVO; Reeta Tarkiainen, TVO; Mikko Tammela, TVO; Gitesh Kumar Patel, LUT; Mikko Ilvonen, VTT; Jaakko Leppänen, VTT)

Approval

VTT TECHNICAL RESEARCH CENTRE OF FINLAND LTD

Date:	27 February 2026
Signature:	Jani Halinen Digitally signed by Halinen Jani 913223442 Date: 2026.02.27 15:43:06 +02'00'
Name:	Jani Halinen
Title:	Vice President, Nuclear energy

Contents

1. Introduction

Critical flow plays a crucial role in nuclear safety analysis. Critical flow occurs when the downstream flow is no longer receiving information from the upstream at the point where the fluid flow velocity approaches the speed of sound. Moreover, when the pressure at the outlet is smaller than the critical value pressure the flow rate through the channel is no longer dependent on the downstream conditions. Thus, quantifying the critical flow is crucial for determining the water injection flow rate from a safety system.

The presented work is related to the critical flow investigation of large length to diameter ratio geometrical configuration which is encountered in steam generators. Thus, the accident associated with such configuration is a steam generator tube rupture (SGTR). SGTR is a design accident that might comprise the reactor integrity if not mitigated. A double break in a steam generator tube reduces the water inventory of the primary circuit and depressurizes the primary side to a point where flashing might occur.

The following work presents a tailored solution to investigate the critical flow in the separate effect test (SET) facility CRiticAl Flow Test facilitY (CRAFTY) test facility constructed in Lappeenranta University of Technology (LUT), in Finland. In previous studies different methods of modeling critical flow were investigated. In [1] a non-homogeneous non-equilibrium model was used showing good agreement between the simulation and the experiment. Thus, similar approach is followed in this work. The solution algorithm used in this work is based on a fully implicit steady state treatment of the six-equation two fluid model (2FM) allowing thermal and mechanical non-equilibrium between the gas and liquid phase.

The algorithm utilizes the Jacobian Free Newton Krylov (JFNK) method to solve the six unknowns $[p, \alpha, u_{\mathrm{GAS}}, u_{\mathrm{LIQ}}, h_{\mathrm{GAS}}, h_{\mathrm{LIQ}}]^T$. The JFNK method requires a good preconditioning scheme in order to reach convergence. The presented work utilizes the numerical library Portable, Extensible Toolkit for Scientific Computation (PETSc)[2]. Thus, the default PETSc finite difference Jacobian was given as a preconditioning matrix[3].

1.1 Modeling of choke flow

The governing equations describing the conservation of mass, momentum and energy of the two-fluid six equation model over a control volume shown in Figure 1 in it's one-dimensional are described by Eq. (1.1)-Eq. (1.3) [4].

Continuity equations:

$$\frac{\partial}{\partial t}\iiint_{\mathcal{V}} \alpha_k \rho_k \, d\mathcal{V} + \iint_S \alpha_k \rho_k u_k \cdot d\mathbf{S} = \iiint_{\mathcal{V}} \Gamma_k d\mathcal{V}, \tag{1.1}$$

momentum equations:

$$\frac{\partial}{\partial t}\iiint_{\mathcal{V}} (\alpha_k \rho_k u_k) \, d\mathcal{V} + \iint_S (\alpha_k \rho_k u_k \cdot d\mathbf{S}) u_k + \iint_S p d\mathbf{S} = \iiint_{\mathcal{V}} M_k d\mathcal{V}, \tag{1.2}$$

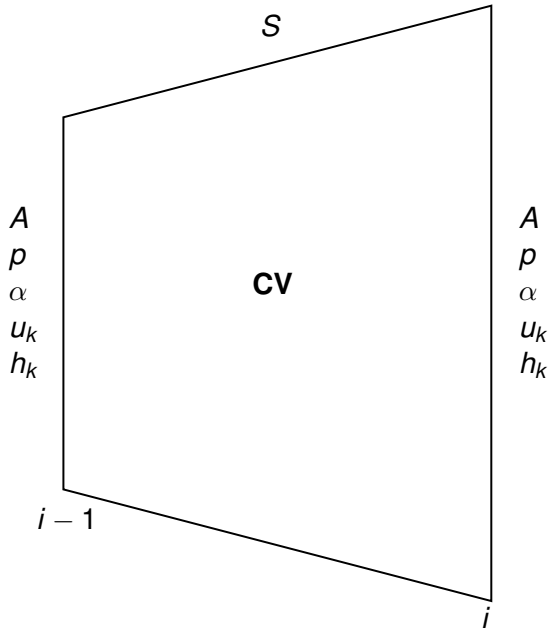

Figure 1. Control volume.

energy equations:

$$\frac{\partial}{\partial t}\iiint_{\mathcal{V}} \alpha_k \rho_k h_k \, d\mathcal{V} + \iint_S \alpha_k h_k \rho_k u_k \cdot d\mathbf{S} = \iiint_{\mathcal{V}} E_k d\mathcal{V} + \frac{\partial}{\partial t}\iint_S \alpha_k p d\mathbf{S}, \tag{1.3}$$

where, the gas and liquid phases denoted by $k \in \{\text{GAS,LIQ}\}$.

Assuming no heat generation and no wall heat transfer. The source terms in the mass, momentum, and energy equations due to interfacial heat transfer, interfacial drag, mass transfer, form losses, wall friction, and gravitational force are summarized in Table 1. Where, for this work the interfacial drag contribution to the energy equation is assumed to be negligible.

Table 1. Governing equations source terms.

Equation	Source term
Continuity equation	Γ_k
Momentum equation	$\Gamma_k u_{ik} + \alpha_k \rho_k g + F_{wk} + F_{ik} + f_k$
Energy Equation	$\Gamma_k h_{ik} + \alpha_k \rho_k u_k g + u_{ik} F_{ik} + Q_{ik}$

The gas and liquid phases follow the following constraints:

$$\Gamma_{\text{GAS}} = -\Gamma_{\text{LIQ}} = -\frac{Q_{i\text{GAS}} + Q_{i\text{LIQ}}}{h_{\text{GAS},sat} - h_{\text{LIQ},sat}}, \tag{1.4}$$

$$F_{i\text{GAS}} = -F_{i\text{LIQ}}, \tag{1.5}$$

$$\alpha_{\text{GAS}} + \alpha_{\text{LIQ}} = 1.0. \tag{1.6}$$

The flow regime assumption is a simple break of the liquid into droplets. Thus, the interfacial heat transfer coefficient for liquid and gas were obtained from Dittus-Boelter. The interfacial friction is based on the generalized equation written as Eq. (1.7). Where, the wall friction factor as function of Reynolds number is computed from Darcy-Weisbach model.

$$F_{i\mathrm{GAS}} = \frac{1}{2} C_d \rho_{\mathrm{GAS}} A_{int} \Delta u |\Delta u|. \tag{1.7}$$

The interfacial heat transfer rate is obtained by Eq. (1.8):

$$Q_{ik} = HTC_k A_{int} (T_{sat} - T_k). \tag{1.8}$$

The interfacial area for droplet flow regime is computed with the assumption that the droplet diameter is 0.65 mm. Moreover, a smooth step function was used to obtain continuous transition when $\lim_{\alpha \to 0} A_{int}$ to avoid a discontinuity that might cause the solution algorithm to fail. The modified interfacial area as function of alpha is shown in Figure 2.

$$A_{int} = \frac{6(1-\alpha)}{d_d}. \tag{1.9}$$

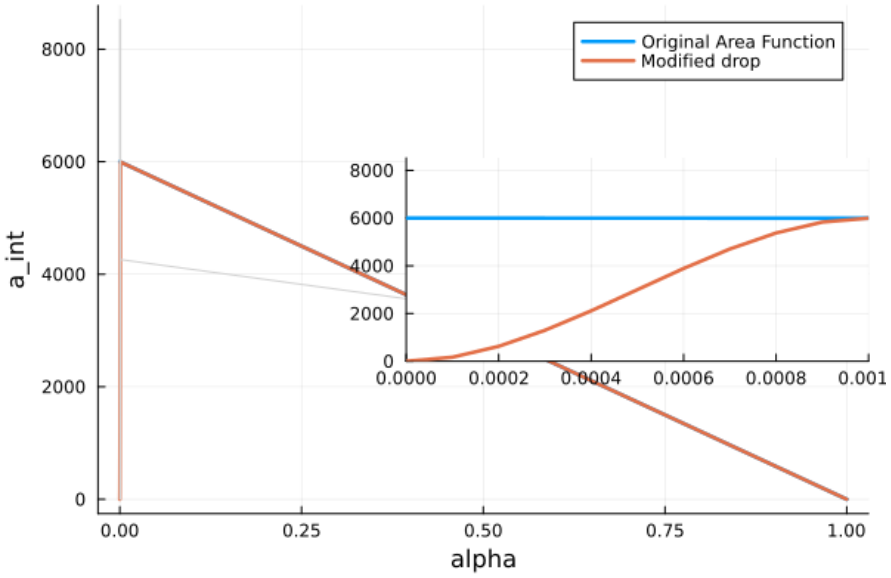

Figure 2. Interfacial area of droplet regime.

2. Solution procedure

Assuming steady state conditions and integrating the governing equation over the CV a marching in space approach can be utilized in order to find the critical flow coupled with a root finding algorithm the bisection method. The continuity and energy equations are obtained in their final form as:

continuity equation:

$$mass_k = (A\alpha_k\rho_k u_k)_i - (A\alpha_k\rho_k u_k)_{i-1} - V_i\Gamma_{k,i}, \tag{2.1}$$

energy equation:

$$energy_k = (A\alpha_k\rho_k u_k h_k)_i - (A\alpha_k\rho_k u_k h_k)_{i-1} - V_i E_{k,i}, \tag{2.2}$$

The momentum equation is integrated with the assumption that the pressure through the side walls is zero. Thus, the final form of the momentum equation reads:

$$momen_k = (A\alpha_k\rho_k u_k^2)_i - (A\alpha_k\rho_k u_k^2)_{i-1} + (A\alpha_k p)_i - (A\alpha_k p)_{i-1} - ((A_i - A_{i-1})(\frac{p_i + p_{i-1}}{2})) - V_i M_{k,i}. \tag{2.3}$$

The nonlinear system of equations at cell i to be solved is summarized as:

$$\mathbf{F}(\mathbf{X_i}) = \begin{bmatrix} mass_{\text{GAS}} \\ mass_{\text{LIQ}} \\ momen_{\text{GAS}} \\ momen_{\text{LIQ}} \\ energy_{\text{GAS}} \\ energy_{\text{LIQ}} \end{bmatrix}_i \tag{2.4}$$

The Newton method at each iteration solves the following linear system [5]:

$$J_F(X_{i,k})s = -F(X_{i,k}), \tag{2.5}$$

$$X_{i,k+1} = X_{i,k} + s, \tag{2.6}$$

where, k is the current iteration and s is the step taken to the next iteration. Instead of computing the analytical Jacobian the JFNK can be used with a finite difference Jacobian as a preconditioner Eq. (2.7).

$$J = \frac{\partial F_j}{\partial x_j} = \frac{F_j(X + \delta x_j) - F_j(X)}{\delta x_j}. \tag{2.7}$$

The six unknowns to be solved at i defined by the vector $X_i = [p, \alpha, u_{\text{GAS}}, u_{\text{LIQ}}, h_{\text{GAS}}, h_{\text{LIQ}}]^T$. Equations of state (EOS) for water and steam are obtained using the IAPWS. Starting from the inlet boundary condition an initial guess is used in the bisection algorithm bounds $[u_{min}, u_{max}]$.

The inlet conditions are propagated through space by marching cell by cell and comparing the last cell called ghost cell pressure with the experiment last reading pressure. The inlet velocity of the boundary condition is adjusted based on the difference between the two pressures in order to get the correct pressure drop. A form loss of value 0.85 is found to give reasonable pressure drop compared with the experiment. The algorithm is briefly summarized in scheme algorithm 1.

Algorithm 1 Outlet pressure matching algorithm

for iter = 1 to $iter_{max}$ **do**
  $u_{in} = 0.5(u_{min} + u_{max})$
  for i = 1 to N **do**
    Solve $F(X_i) = 0.0$
  end for
  if $|P_N - P_{exp}| \leq \epsilon$ **then**
    break
  else
    if $P_N > P_{exp}$ **then**
      $u_{min} = u_{in}$
    else
      $u_{max} = u_{in}$
    end if
  end if
end for

3. CRAFTY experiment

The CRAFTY test facility shown in Figure 4. The facility is modular in a way that experiments with different tube lengths and diameters can be conducted by replacing the discharge tube. A scram tank filled with water pressurized by Nitrogen through the "Gas manifold" shown in Figure 4 is used to mimic the pressure of the primary side of a steam generator in a Pressurized Water Reactor (PWR). The maximum pressure and temperature in the scram tank are 100 bar and 270 °C respectively. The pressurized water in the scram tank go though a U-bend before entering the discharge tube. Where, the flow through the discharge tube shown in Figure 3 is expected to reach critical flow due to the depressurization and the area change. Finally, the flow through the discharge tube leaves the system into a large vessel "PPOOLEX".

Figure 3. Discharge tube from the U-tube to the PPOOLEX [6].

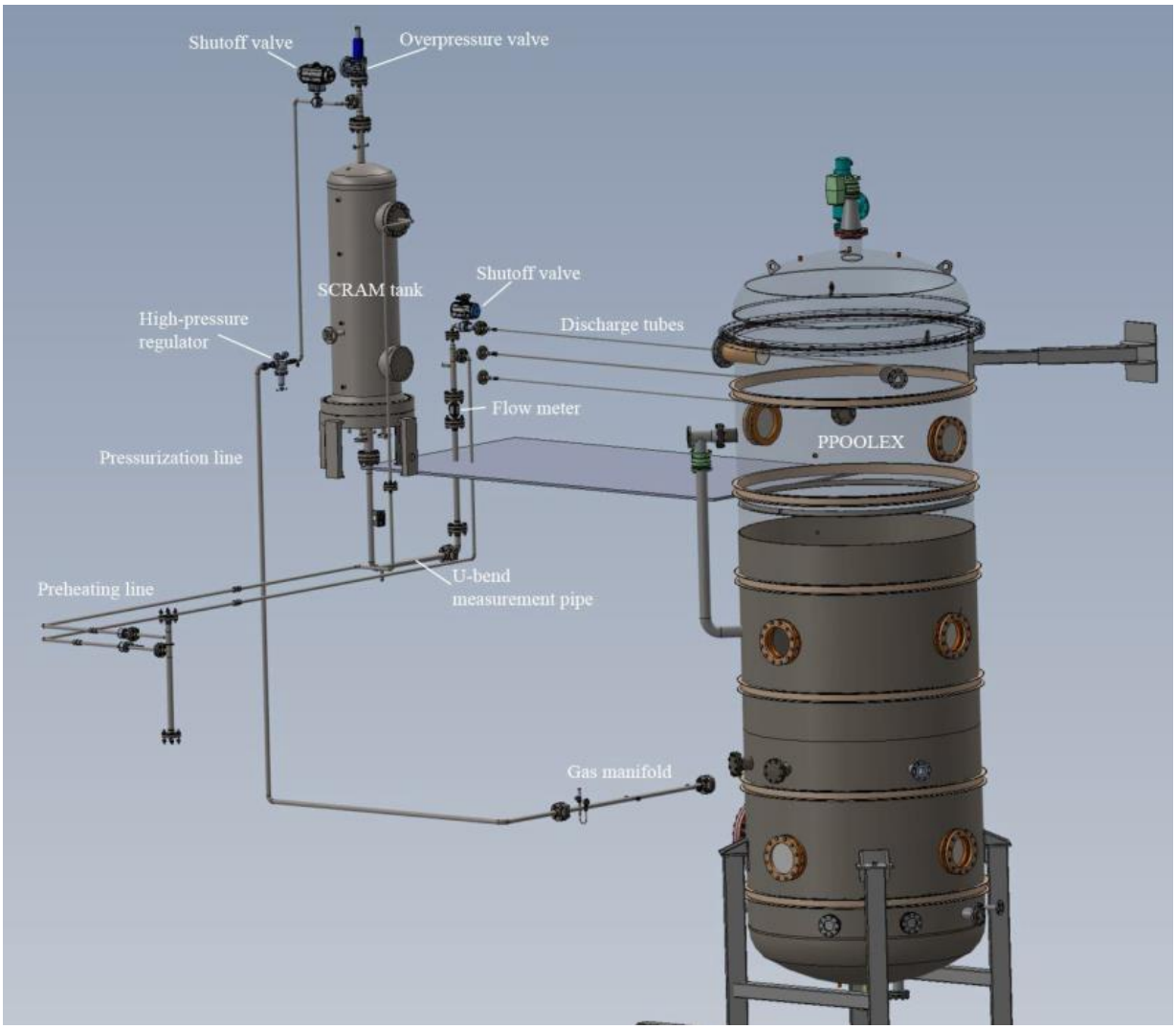

Figure 4. CRAFTY configuration [6].

3.1 CRAFTY model

Figure 5 shows the simulation discretization. The number of cells and cell sizes shown in the figure do not represent the actual numbers used. The model assures smooth area change in the regions where the diameter of the pipe changes in order to avoid sharp increase or decrease in the pressure gradient. Form losses were given for the elbows of a value of 0.22. The different inlet conditions used are summarized in Table 2. The discharge tube diameter used was 13 mm.

Table 2. Boundary conditions.

Experiment	Temperature °C	Pressure bar
POC4	267.6498	60.4895
POC5	268.8159	84.7062

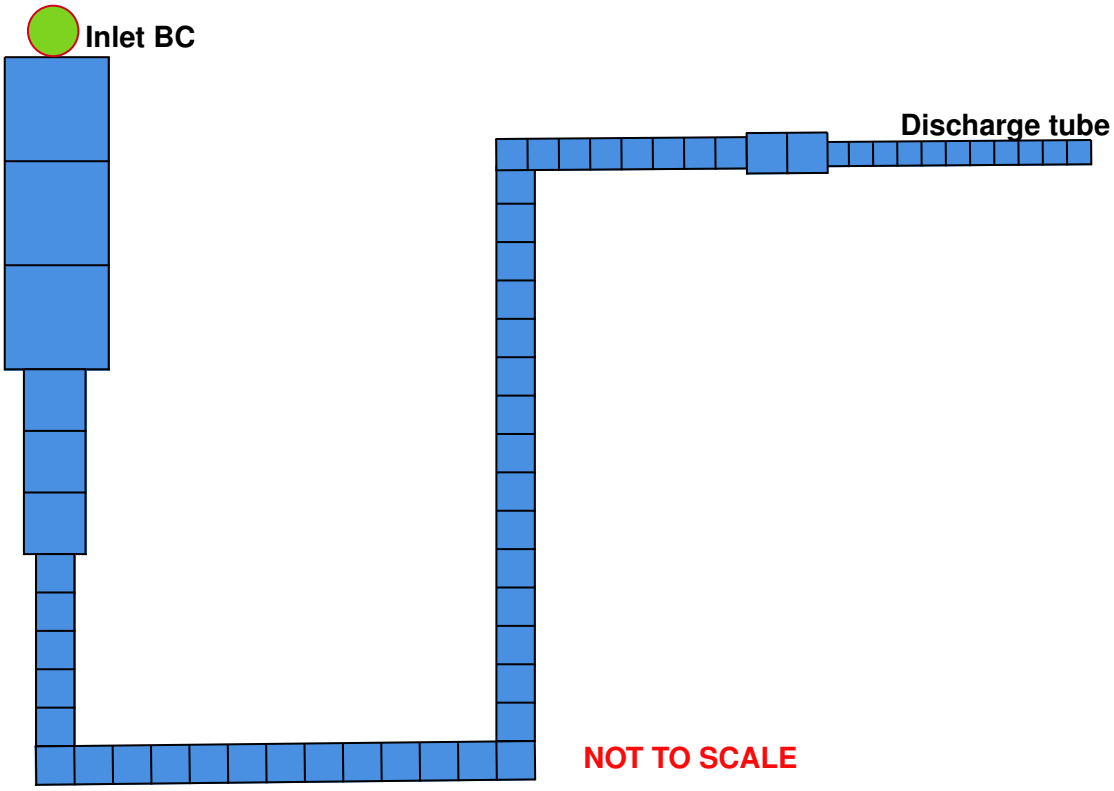

Figure 5. Schematic representation of the calculation mesh for CRAFTY facility.

4. Results

The pressure profile in the discharge tube using the experiment **POC4** boundary conditions is shown in figure Figure 6a. During the single phase region the simulation and the experimental results are quantitatively in agreement. However, for the two phase region starting from 2m the flashing causing the pressure drop in the experiment takes place around 3m where for the simulation the phase change occur around at the very end of the discharge tube. Moreover, the experiment pressure drop caused by the acceleration due to flashing is larger compared to the simulation. The temperature profile is shown in figure Figure 6b.

The temperature stays constant until phase change occurs. The temperature profile during the single phase is in agreement with the experiments. Thus, the heat losses through the wall to the surrounding can be concluded to be small. In the simulation the temperature drop is underestimated compared to the experimental data. One potential reason can be because of the lack of the wall heat transfer in the simulation which is reflected on smaller temperature drop.

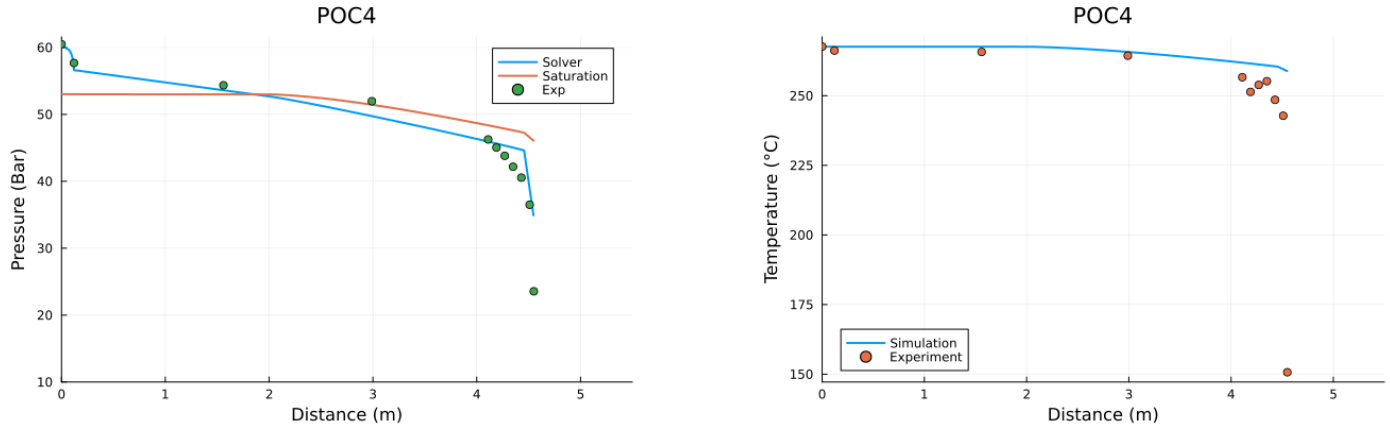

(a) Pressure profile POC4 **(b) Temperature profile POC4**

Figure 6. POC4 results

For **POC5** the pressure profile is shown in figure Figure 7a. The **POC5** pressure results of the simulation show better agreement with the experimental data than in the **POC4**. During the single phase region the experimental and the simulation pressure distribution is in perfect quantitative and qualitative agreement. However, similar to the **POC4** the pressure drop at the end of the discharge tube takes place at shorter distance in the experiment while for the simulation it is closer to the end of the discharge tube.

The temperature profile is shown in Figure 7b. During the single phase region the temperature distribution of the simulation and the experiment have the same qualitative behavior. Heat losses to the surrounding is low when compared to the energy passing through and ejecting from the system (or discharge tube). However the temperature drop is again underestimated by the simulation in a similar manner when phase change from a single to two phase region occurs near the end of the discharge tube.

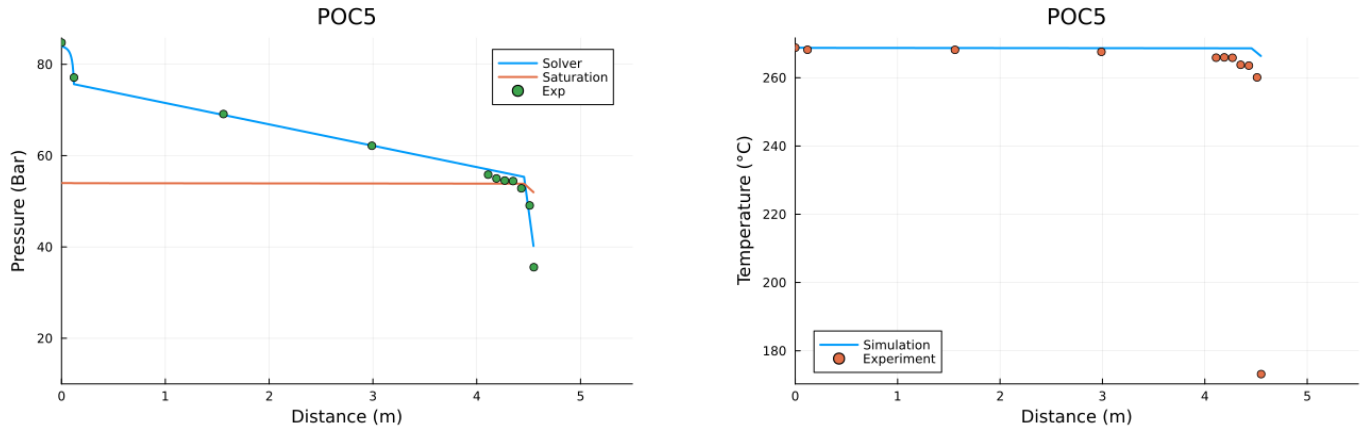

(a) Pressure profile POC5 **(b) Temperature profile POC5**

Figure 7. POC5 results

The mass flux at the end of the discharge tube in the simulation compared to the Moody mass flux is shown in Table 3. Based on the mass flux comparison and the presented results the pressure drop at the end of the discharge tube is governed by the acceleration of fluid due to the flashing. Thus, the flow did not reach critical conditions.

Table 3. Critical mass flux comparison.

Experiment	Simulation mass flux $kg \cdot s^{-1} \cdot m^{-2}$	Moody mass flux $kg \cdot s^{-1} \cdot m^{-2}$
POC4	23682.7861	31364.2715
POC5	37440.8596	52474.5504

5. Conclusion

In the presented work simulation of the SET CRAFTY was performed in order to investigate critical flow. A simple droplet flow regime is assumed as a first guess to formulate the interfacial area. A steady state in-house developed code with fully implicit scheme using backward finite difference spatial discretization was used to solve the governing equations based on the two-fluid non-equilibrium model. The JFNK method was utilized with the finite difference Jacobian supplied as a preconditioner. The results presented show qualitative agreement in pressure distribution for the experiment with higher pressure boundary condition.

Temperature profiles showed good agreement up until the point where a phase change starts to occur where simulation overestimates the temperature profile. One of the reasons for the differences in temperature can be due to lack of wall heat transfer modeling. The presented work relying on the experimental data provided with simple assumptions show that the flow did not reach critical conditions.

The presented work is meant as a first step for analyzing experimental data in a steady-state fashion. Thus, further development and enhancement such as adding wall heat transfer and more detailed flow regimes to the solver will be considered when new experimental data is available. There are future plans of having transparent discharge tubes in the experiment which would allow formulating more complex closure laws based on the flow regimes distribution.

Bibliography

[1] X. Hong, B. Aurelian Florin and C. Xu. Development of a new full-range critical flow model based on non-homogeneous non-equilibrium model. In: Annals of Nuclear Energy 158 2021, p. 108286.

[2] S. Balay et al. PETSc Web page. http://www.mcs.anl.gov/petsc. 2015.

[3] L. Zou, H. Zhao and H. Zhang. Implicitly solving phase appearance and disappearance problems using two-fluid six-equation model. In: Prog. Nucl. Energy 88 2016, pp. 198–210.

[4] M. Ishii and T. Hibiki. Thermo-fluid dynamics of two-phase flow. Springer, 2006.

[5] E. Bueler. PETSc for Partial Differential Equations: Numerical Solutions in C and Python. Society for Industrial and Applied Mathematics, 2020.

[6] L. Pyy et al. GENERAL DESCRIPTION OF CRAFTY - FIRST EDITION. Lappeenranta, Finland: Lappeenranta-Lahti University of Technology LUT School of Energy Systems Nuclear Engineering, 2023.